Measurement of the dynamic deformation of a high frequency scanning mirror using a Shack-Hartmann wavefront sensor

Margaret Brown,[a*] Timothy Gong,[a] Daniel R. Neal,[b**] James Roller,[b] Selso Luanava[a] and Hakan Urey[a]

[a]Microvision Inc., 19910 North Creek Parkway S., Bothell, WA 98011

[b]WaveFront Sciences, 14810 Central Ave SE, Albuquerque, NM 87123

ABSTRACT

Scanning mirrors for micro-display systems typically require operation at frequencies over 15 kHz. These mirrors undergo large dynamic stresses and inertia related deformations. We report here on the measurement of these dynamic deformations using a commercially available Shack-Hartmann wavefront sensor with data reduction software. The measured deformations using the Shack-Hartmann wavefront sensor are shown to agree with measurements obtained using a stroboscopic interferometer. Advantages of the Shack Hartmann wavefront sensor are discussed.

1. INTRODUCTION

The dynamic deformation of high frequency optical scanning mirrors limits system optical resolution by imposing wavefront errors on the scanning optical beam that ultimately result in an increase in the smallest achievable optical spot.[1,2,3] To achieve a mirror design with a minimum dynamic deformation, the approach taken here is to optimize the design using a detailed finite element analysis (FEA) of the mechanical design of the mirror structure. The mirror is then fabricated and the wavefront deformation measured. Measurements are compared with the FEA predictions and used to improve subsequent mirror designs. This design process requires routine, accurate and reliable measurements of the mirror deformation.

Two different instruments have been used to measure the dynamic deformation of our optical scanning mirrors. The first instrument is a custom-built stroboscopic interferometer [4] with custom designed data reduction software to infer the mirror deformation. This instrument performed with a high spatial resolution and a noise floor estimated to be ~λ/10. However, the collection and reduction of data is time consuming. To facilitate the rapid measurement and analysis of the dynamic deformation of the scanning mirrors, we replaced the stroboscopic interferometer with a commercially available Shack-Hartmann wavefront sensor. This instrument enabled routine and accurate dynamic deformation measurements while maintaining the sensitivity and accuracy of the stroboscopic interferometer.

In this paper, we summarize the theoretical predictions of the dynamic deformation developed from the FEA. We then describe the experimental test beds and procedures for both the interferometer and Shack-

* Margaret_brown@mvis.com; phone 425-415-6779; fax 425-415-6601; http://www.mvis.com; Microvision Inc, P.O. Box 3008, Bothell, Wa 98011;

** drneal@wavefrontsciences.com; Ph: (505) 275-4747 (X107);Fax: (505)275-4749; : http://www.wavefrontsciences.com; WaveFront Sciences, Inc.,14810 Central S.E. , Albuquerque, NM 87123

Optical Manufacturing and Testing IV, H. Philip Stahl, Editor, Proceedings of SPIE Vol. 4451 (2001)

Hartmann wavefront sensor measurements. The measurements and FEA analysis predictions are then compared.

2. SHACK-HARTMANN SENSOR

The Shack Hartmann sensor and data acquisition and reduction software used here is a model CLAS-2D manufactured by Wavefront Sciences.[5] A discussion of the theoretical operation and data reduction process can be found in various papers.[5,6,7] A brief summary is presented here.

2.1 Theory of Operation

Shack-Hartmann wavefront sensors were developed originally for adaptive optics applications.[8,9] However, with the development of micro-optics based lenslet arrays and high-resolution CCD cameras, their use has been extended to a wide variety of applications.[5,6,10] The sensor is compact, robust and inherently simple. It is based on the simple principle that light propagates normal to the wavefront surface. Thus changes in focal spot position on the CCD array provides a direct measure of wavefront slope, and through a spatial integration process, the wavefront can be determined.

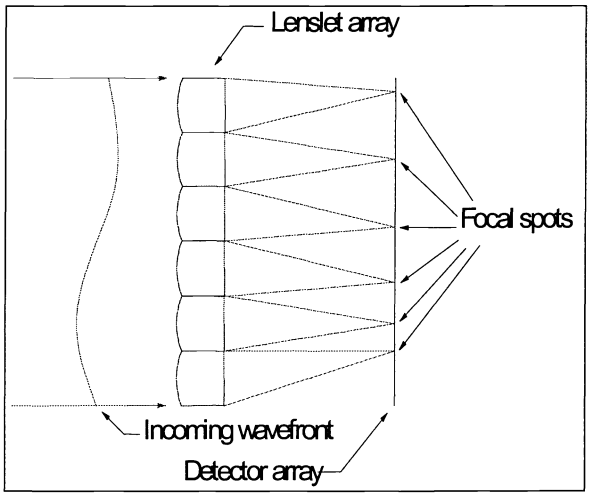

Figure 1- A wavefront incident on the lenslet array will produce distinct focal spots on the CCD. The location of these focal spots relative to a reference is a measure of the local wavefront tilt at the lenslet array.

The Shack-Hartmann sensor consists of a micro-optic lenslet array that is rigidly mounted in front of a CCD detector as shown in Figure 1. The fused silica lenslet array is made using photo-lithography and etching processes, with 1 μm resolution feature sizes. Each of the lenslets is a precision asphere arranged in a rectangular array with 100% fill factor. The wavefront sensor used here consists of a 10 bit CCD camera with a 33 x 44 lenslet array across a 4.8 x 6.4 mm aperture.

The lenslet array creates a series of focal spots on the detector array. With appropriate synchronization between the scan mirror, diode laser source and camera electronics, the CCD records the location of the focal spots and transfers them to the computer memory. This information is processed using the procedure shown schematically in Figure 2. First the CCD image is generated representing the distribution of power across the detector. Each focal spot is then located and the location of the centroid corresponding to each lenslet is calculated. The wavefront slopes can then be calculated from the difference between these centroid locations and those of a reference wavefront. The wavefront is then reconstructed from the wavefront slopes.

The use of the reference file allows for the minimization of effects from imperfections in the CCD array, lenslet array, mounting system, imaging systems and electronics. The reference file is determined by recording the position of the focal spots at a known condition.

The Shack-Hartmann wavefront sensor has both a large dynamic range (4-5 mrad/lenslet) and a high sensitivity ($<\lambda/20$ Peak to Valley), that allow capture of wavefront measurements over a wide range of mirror angles, since measurements of the scanning mirror can be made when there is a relatively large residual tilt in the wavefront.

3. FINITE ELEMENT ANALYSIS OF MIRROR DEFORMATION

The basic structure of the scanning mirror is illustrated in the left panel of Figure 3. The mirror is rotated by twisting at the torsion bars, shown here at the top and bottom of the mirror. Previous attempts to model the mirror deformation were performed using 2-D models[2] that calculated the deformation at the centerline of the mirror and then extrapolated this into 3-D space. However, using this centerline approximation, it was impossible to see the effects of the dominant deformation mechanism due to twisting at the torsion bars on the mirror.

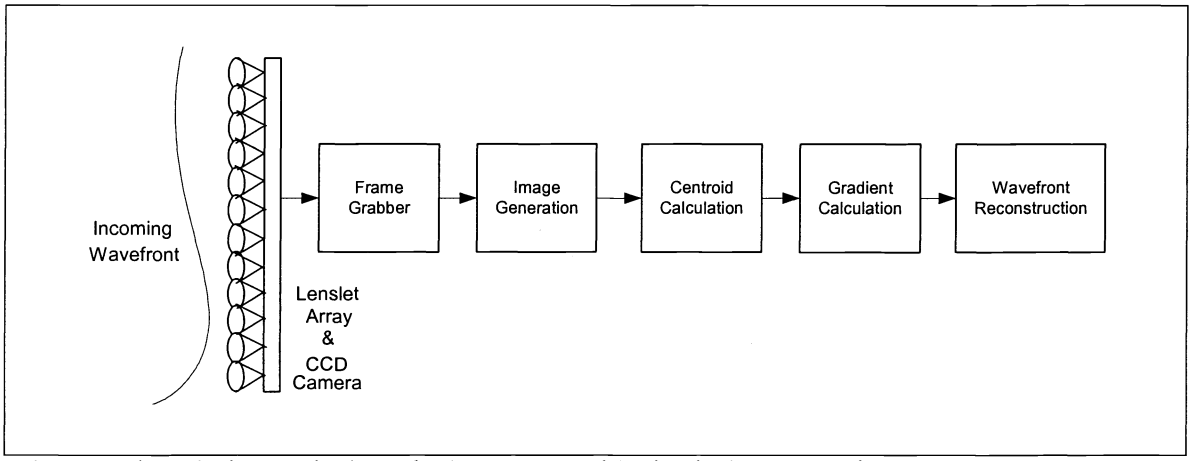

Figure 2- Schematic showing the data reduction process used for the Shack-Hartmann device.

FEA allowed us to model the characteristic deformation at the torsion beam and the "flapping" of the corners of the mirror. The FEA program used to model and analyze the mirror deformation is Cosmos/M. The FEA predicted surface deformation was multiplied by a factor of 2 to obtain the wavefront deformation and is plotted here in the right panel of Figure 3. For a 1.27 degree maximum scan angle, the predicted peak to peak wavefront deformation is 0.44 λ with an RMS error of 0.059 λ. This data is compared with measurements of the same mirror, summarized in subsequent sections of this paper, and found to be about 25% larger than the measured deformation. We believe this is due to uncertainty in the damping coefficient used in the FEA. Measurements confirm the dominant deformation mechanisms to be the stress at the torsion beam and the flapping at the corners.

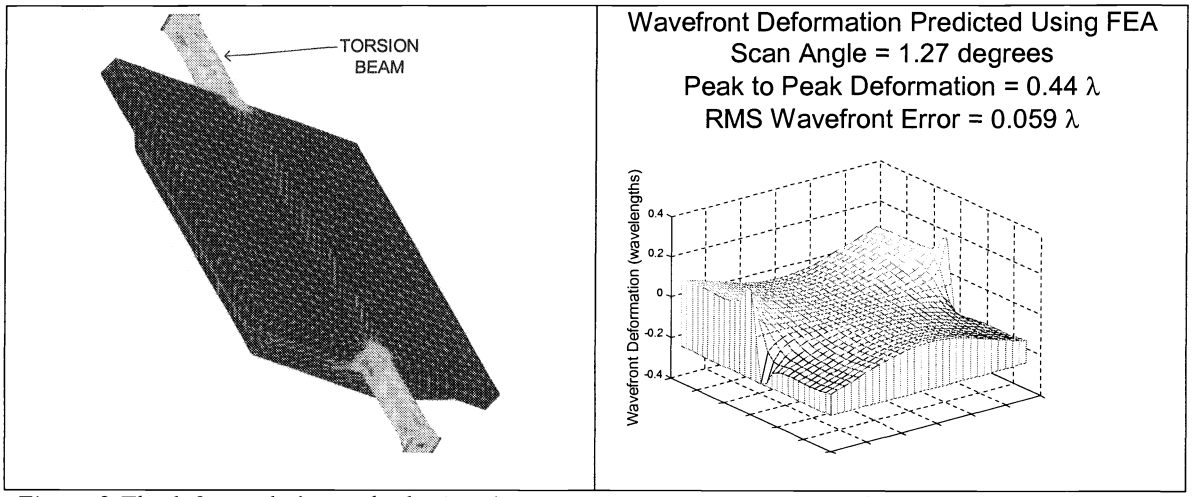

Figure 3-The left panel shows the basic mirror structure. Rotation occurs about an axis parallel to and running through the torsion beams. The right panel shows the results of the FEA. Deformation is dominated by twisting stress at the torsion beams.

5.1 EXPERIMENTAL DESIGNS

4.1 Stroboscopic Interferometer

A schematic of the stroboscopic interferometer is shown in Figure 4. A Twyman-Green interferometer is formed using a beam splitter, reference mirror and the scanning mirror. A fiber coupled 635 nm laser diode is used as the light source and a relay imaging system is used to image the fringe pattern onto the CCD camera. Fiber coupling is used here to provide a diffraction limited optical beam. A maximum of 2 mw of power is delivered from the fiber.

The scanning mirror is driven in a sinusoidal oscillation at between 15 and 20 kHz and at maximum angles ranging from 0 to over 5 degrees. To facilitate the measurement of the dynamic mirror deformation at an arbitrary scan angle, a signal is synchronized to the phase of the scanning mirror and is delivered to a delay generator, which in turn delivers a pulse to the laser diode driver at the frequency at which the scanning mirror is oscillating. Adjustment of the delay tunes the strobe to be incident on the scanning mirror at a specific scan angle. The rotation stage then redirects the beam that is reflected at the scanning mirror down the optical axis of the interferometer on into the CCD camera.

The duration of the laser pulse determines the temporal resolution of the measurement. Minimizing the pulse length increases the temporal resolution of the measurement. However, this reduces the power incident on the CCD camera resulting in poor contrast and a low signal to noise ratio. The measurement presented here used pulse durations between 10-20 nsec.

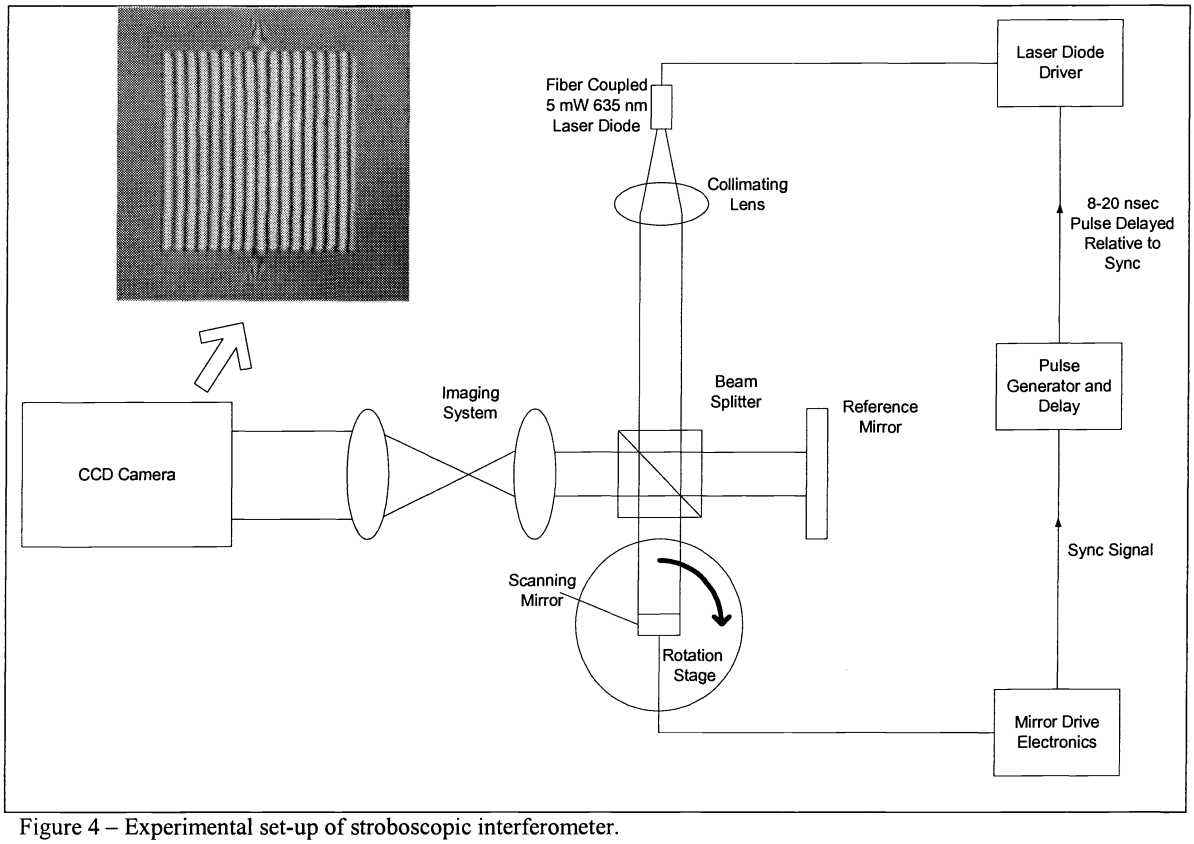

Figure 4 – Experimental set-up of stroboscopic interferometer.

A spatial linear carrier analysis[13] reduces the interferogram and the surface deformation of the mirror is inferred. A carrier frequency is introduced by tilting the reference wavefront relative to the sampling wavefront, introducing high spatial frequency fringes into the interferogram. The typical frequency of the spatial carrier for the data taken is ~ 10 (mm^{-1}). High frequency noise is removed using a low pass filter

with a cut-off frequency set to .75 times the carrier frequency. A typical interferogram taken from a MEMs scanning mirror is shown in the upper left corner of Figure 4.

4.2 Shack-Hartmann Wavefront Sensor

The experimental set-up for the Shack-Hartmann is similar to the interferometer. Figure 5 shows a schematic of the test bed. The Shack-Hartmann test bed uses the same laser diode and electronics with the same delay and triggering schemes used in the interferometer. Here we have not fiber coupled the laser diode. This allows us to deliver more power to the Shack-Hartmann sensor, reducing the integration time on the CCD camera and increasing the temporal resolution. Because the Shack-Hartmann data reduction software can remove wavefront errors on the reference beam, a perfect diffraction limited beam was not required. The rotation stage, enables sampling the dynamic mirror deformation at arbitrary scan angles.

The measurement procedure requires that the Shack-Hartmann wavefront sensor be located at the image plane of the imaging system and that the scanning mirror be located at the object plane. With this condition met, rotation of the mirror will not result in a lateral translation of the image plane. The alignment procedure begins with the scanning mirror in a static position. The surface of the mirror is mounted such that is located directly above the center of rotation of the rotation stage. A translation stage enables fine adjustment of the mirror surface relative to the center of rotation. Alignment of the reflected beam is such that it is coincident with the optical axis of the imaging system and directed onto the center of the sensor. The longitudinal position of the sensor is adjusted using a translation stage such that the image of the scanning mirror remains stationary as static mirror is rotated. The position of the object plane is then verified by rotating the static mirror. If the camera is located at the image plane and the scanning mirror is located at the object plane, there will be no lateral translation of the image as the mirror is rotated. Some iteration is required to minimize the translation.

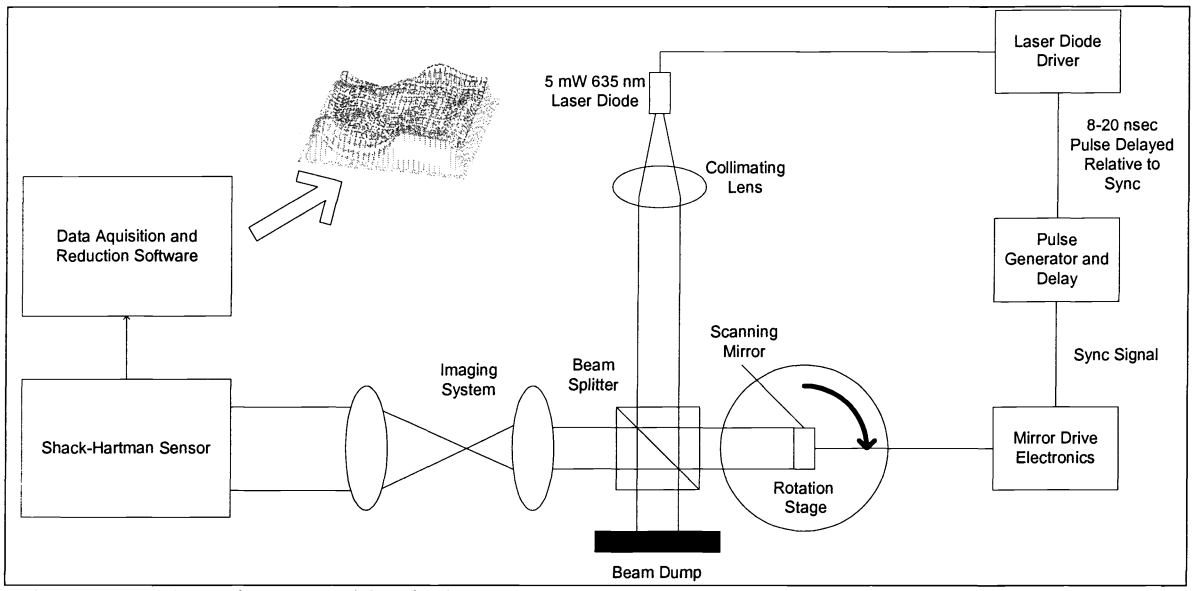

Figure 5- Experimental set-up used for Shack-Hartmann wavefront sensor measurements.

To create reference wavefront data, the scanning mirror is returned to its static position with the reflected beam directed down the optical axis of the imaging system and a reference beam is recorded. Typical noise floors, achieved in this way, are less than 0.05 λ. Note here that the creation of the reference file in this way, removes any static surface deformation from the mirror. To check the repeatability of this noise floor, the scanner was turned on and off several times, and the noise floor measured. We found that the noise floor returned to less than 0.05 λ.

The next step in the measurement procedure is to turn the scanner on and adjust the delay on the laser diode pulse until the measured wavefront tilt is minimized. This results in the condition that the laser pulse

samples the mirror at a zero scan angle. The data acquisition and reduction software operates rapidly and is able to provide effectively "real time" measurements of the wavefront tilt as the delay is tuned.

After determining the delay at the center of the scan, incremental changes in the delay are made. Changing the delay results in the introduction of a wavefront tilt. The software displays the magnitude of this tilt. The rotation stage is now used to remove the tilt. As the tilt of the mirror is removed, the dynamic surface deformation of the mirror is displayed. Complete removal of the tilt is not necessary, as the software will subtract tilt (if it does not exceed the dynamic range of the instrument). In this way, a surface deformation map of the mirror surface is measured at a known angle of the scanner oscillation.

5.1 RESULTS

In this section, we present wavefront deformation measurements for a MEMS mirror. Measurements are taken of the same mirror using both the interferometer and the Shack-Hartman. Results show good agreement with the FEA results, confirming the dominant deformation mechanism. Further, the results obtained using the interferometer are in excellent agreement with those obtained using the Shack-Hartmann wavefront sensor.

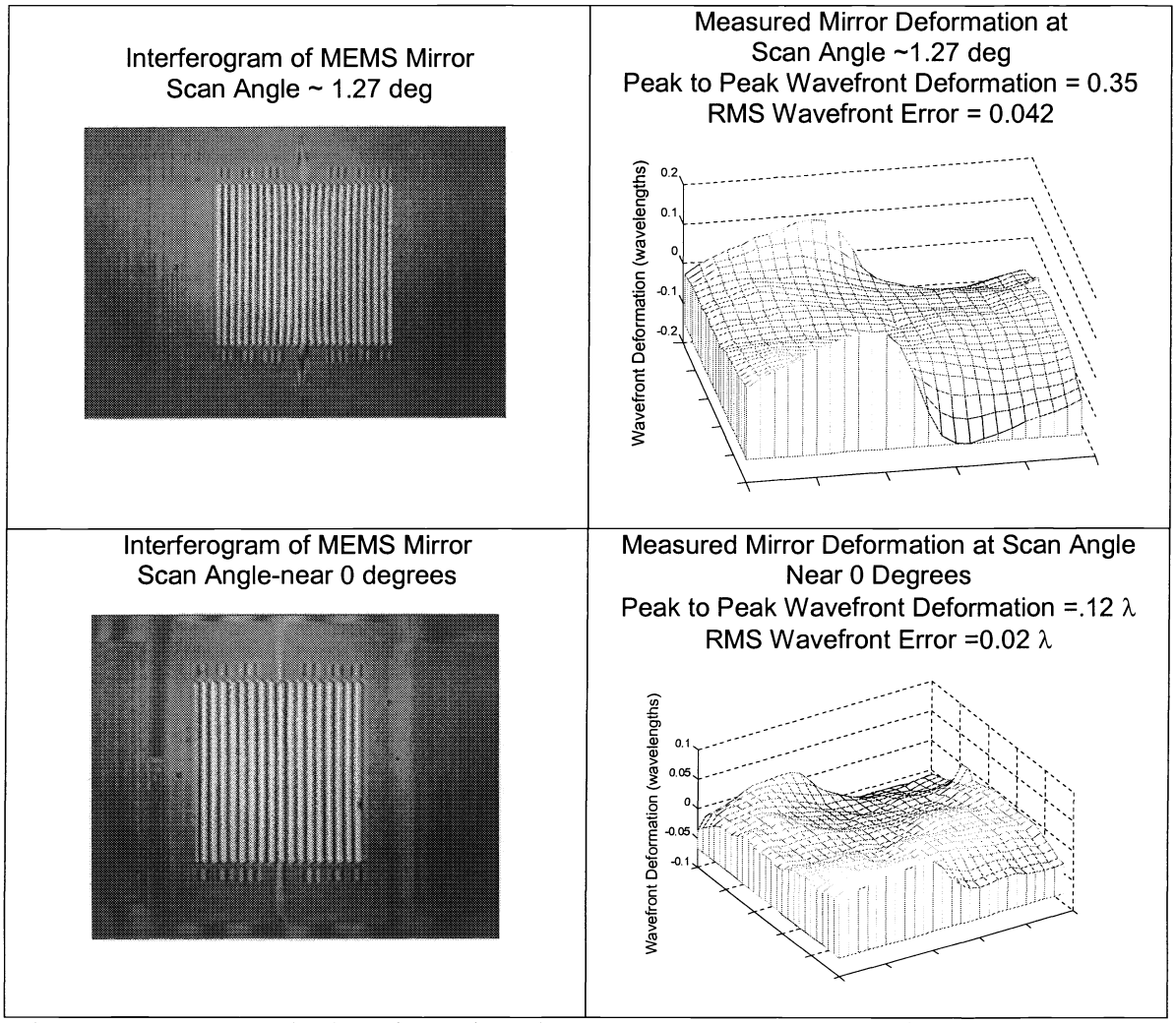

Figure 6- Measurement results obtained using the stroboscopic interferometer. Results are shown for scan angles at 0 and 1.27 degrees.

5.1 Interferometric Measurements

The MEMS mirror is mounted as described previously onto the rotation stage of the interferometer test bed. Two interferograms are taken, one with the delay set at the peak voltage of the drive electronics and one with the delay set at a zero crossing of the drive electronics. There is some delay between the peak voltage and the scan angle due operation at resonance and delays in the electronics.

The left panel of Figure 6 show these data. The wavefront deformation maps, inferred from the interferograms, are shown on the right panels. Peak to peak wavefront deformation at a scan angle estimated to be 1.27 degrees, is calculated to be 0.35 λ with an RMS wavefront error of 0.042 λ. The deformation map shows the characteristic warping due to stress at the mirror flexures predicted by the FEA.

The lower panels show the results for a scan angle near zero. At a zero scan angle the mirror acceleration is zero and the mechanical stresses are zero. In this case, the wavefront deformation should indicate no warping at the flexures. However, this deformation map shows clear warping due to stresses, from which we conclude that the scan angle is not at precisely zero. Given the clear indication of this characteristic peak to peak deformation, we conclude that the interferometer is capable of resolving features with a sensitivity greater than 0.05 λ.

5.2 Shack Hartmann Wavefront Sensor Measurements

The same scanning mirror is measured using the Shack-Hartmann device and using the procedure described above. The left panel of Figure 7 shows the results for a scan angle of 1.27 degrees. The surface map shows the characteristic dynamic deformation of the torsion beams. The magnitude of the peak to peak wavefront deformation is measured to be 0.32 λ with a RMS wavefront error of 0.046 λ. Both of which are in good agreement with the interferometer measurements. The results in the right panel show the mirror deformation at a scan angle of 6.5 deg. The measured peak to peak wavefront deformation is 1.34 λ with a RMS error of 0.19 λ.

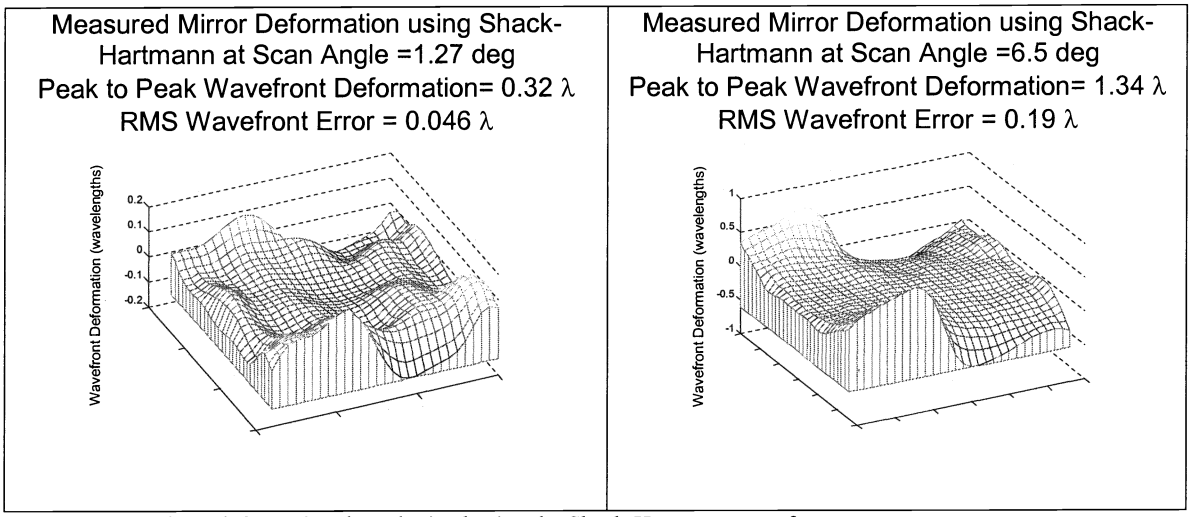

Figure 7-Wavefront deformation data obtained using the Shack-Hartmann wavefront sensor.

6.0 Conclusions

The dynamic deformation of a high frequency MEMS scanning mirror has been modeled using FEA and measured using an interferometer and a Shack-Hartmann wavefront sensor. Measurements using the interferometer and Shack-Hartmann are in excellent agreement. Measurements confirm that the dominant deformation mechanism is twisting at the mirror torsion beams. Measurements are about 25% less than

that predicted by the FEA. We believe this is due to uncertainty in the damping coefficients used in the FEA.

Both the Shack-Hartman sensor and the stroboscopic interferometer have been shown to be capable of measuring high frequency mirror deformations with a sensitivity of less than .05 λ. Advantages of the Shack-Hartmann device include; 1) a robust production ready measurement package; 2) the near real time data reduction software enabling rapid measurements; 3) the use of a reference file enabling the removal of aberrations in the probe beam and imaging optics; and 4) a large dynamic range allowing for accurate location of the mirror angle.

Improvements that will be made to the test bed using the Shack-Hartmann wavefront sensor include increasing the laser diode power. A 200 mW 830 nm laser diode has recently been installed on the test bed. This will allow for shorter integration times and higher temporal resolution, with the possibility of performing single shot measurements. The resolution of the rotation stage will be increased allowing for the adjustment and measurement of the scan angle with higher precision.

REFERENCES

1. Urey, H.; Wine, D.; Osborn, T. Optical performance for MEMS-scanner based microdisplays. In *MOEMS and Miniaturized Systems*, Proc. SPIE vol. 4178, Santa Clara, CA, Sep 2000,176-185.

2. Urey, H.; Wine, D.W.; Lewis, J. R. Scanner design and resolution tradeoffs for miniature scanning displays. In *Flat Panel Display Technology and Display Metrology*, Proc. SPIE vol. 3636, San Jose, CA, Jan. 1998; 60-68.

3. R. Conant, J. Nee, K. Lau, R. Muller, "Dynamic Deformation of Scanning Micromirrors," IEEE/LEOS Optical MEMS 2000, Kauai, Hawaii, pgs 49-50.

4. J.S. Harris, R.L. Fusek and J.S. Marcheski, "Stroboscopic interferometer", Applied Optics, 18, 2368-2371, 1979

5. D. R. Neal, D. J. Armstrong and W. T. Turner, "Wavefront sensors for control and process monitoring in optics manufacture," SPIE **2993** (1997)

6. D. R. Neal, W. J. Alford, and J. K. Gruetzner, "Amplitude and phase beam characterization using a two-dimensional wavefront sensor," SPIE Vol. **2870**, pp. 72–82 (1996).

7. W. H. Southwell, "Wave-front estimation from wave-front slope measurements," J. Opt. Soc. Am., Vol. **70**, No. 8 (August 1980).

8. R. Q. Fugate, "Observations of faint objects with laser beacon adaptive optics," SPIE Vol. **2201**, pp. 10–21 (1994).

9. D. R. Neal, T.J. O'Hern, J.R. Torczynski, M.E. Warren, and R. Shul, "Wavefront sensors for optical diagnostics in fluid mechanics: application to heated flow, turbulence and droplet evaporation," SPIE Vol. **2005**, pp. 194-203 (1993).

10. D. R. Neal, W. J. Alford, and J. K. Gruetzner, "Amplitude and phase beam characterization using a two-dimensional wavefront sensor," SPIE Vol. **2870**, pp. 72–82 (1996).

11. D. R. Neal, D. J. Armstrong, E. Hedlund, M. Lederer, A. Collier, C. Spring, J. Gruetzner, G. Hebner and J. Mansell, "Wavefront sensor testing in hypersonic flows using a laser-spark guide star," SPIE Vol. **3172**-36 (1997).

12. D. R. Neal, D. J. Armstrong and W. T. Turner, "Wavefront sensors for control and process monitoring in optics manufacture," SPIE **2993** (1997)

13. D. Malacara, M. Servin, and Z. Malacara, "Interferogram analysis for optical testing", pg 299-300 Marcel Dekker, Inc, New York, NY, 1998